IVYSPRING INTERNATIONAL PUBLISHER

Theranostics

2018; 8(21): 5814-5827. doi: 10.7150/thno.28252

Research Paper

A heparan sulfate-based matrix therapy reduces brain damage and enhances functional recovery following stroke

Yacine Khelif[1], Jérôme Toutain[1], Marie-Sophie Quittet[1], Sandrine Chantepie[2], Xavier Laffray[2], Samuel Valable[1], Didier Divoux[1], Fernando Sineriz[3], Emanuelle Pascolo-Rebouillat[3], Dulce Papy-Garcia[2], Denis Barritault[2,3], Omar Touzani[1*], Myriam Bernaudin[1✉*]

1. Normandie Univ, UNICAEN, CNRS, CEA, ISTCT/CERVOxy group, GIP CYCERON, 14000 Caen, France
2. CRRET (EA 4397/ERL CNRS 9215), Université Paris-Est, Université Paris Est Créteil, 94010 Créteil, France.
3. Société OTR3, 4 rue Française, 75001 Paris, France.

* Authors contributed equally to the work

✉ Corresponding author: bernaudin@cyceron.fr

Received: 2018.07.02; Accepted: 2018.10.12; Published: 2018.11.12

Abstract

Alteration of the extracellular matrix (ECM) is one of the major events in the pathogenesis of brain lesions following ischemic stroke. Heparan sulfate mimetics (HSm) are synthetic pharmacologically active polysaccharides that promote ECM remodeling and tissue regeneration in various types of lesions. HSm bind to growth factors, protect them from enzymatic degradation and increase their bioavailability, which promotes tissue repair. As the ECM is altered during stroke and HSm have been shown to restore the ECM, we investigated the potential of HSm4131 (also named RGTA-4131®) to protect brain tissue and promote regeneration and plasticity after a stroke.

Methods: Ischemic stroke was induced in rats using transient (1 h) intraluminal middle cerebral artery occlusion (MCAo). Animals were assigned to the treatment (HSm4131; 0.1, 0.5, 1.5, or 5 mg/kg) or vehicle control (saline) groups at different times (1, 2.5 or 6 h) after MCAo. Brain damage was assessed by MRI for the acute (2 days) and chronic (14 days) phases post-occlusion. Functional deficits were evaluated with a battery of sensorimotor behavioral tests. HSm4131-^{99m}Tc biodistribution in the ischemic brain was analyzed between 5 min and 3 h following middle cerebral artery reperfusion. Heparan sulfate distribution and cellular reactions, including angiogenesis and neurogenesis, were evaluated by immunohistochemistry, and growth factor gene expression (VEGF-A, Ang-2) was quantified by RT-PCR.

Results: HSm4131, administered intravenously after stroke induction, located and remained in the ischemic hemisphere. HSm4131 conferred long-lasting neuroprotection, and significantly reduced functional deficits with no alteration of physiological parameters. It also restored the ECM, and increased brain plasticity processes, i.e., angiogenesis and neurogenesis, in the affected brain hemisphere.

Conclusion: HSm represent a promising ECM-based therapeutic strategy to protect and repair the brain after a stroke and favor functional recovery.

Key words: Neuroprotection, extracellular matrix, functional recovery, stroke, heparan sulfate mimetics.

Introduction

Stroke remains a major health and economic problem worldwide. Presently, thrombolysis and thrombectomy are the only available treatments during the acute stage of ischemic stroke. Although

the therapeutic window has been extended for both treatments [1], it remains very narrow for thrombolysis with the recombinant tissue plasminogen activator (rt-PA; < 4.5 hours), which is therefore given to a minority of patients [2]. Thus, there is still an urgent need of developing new treatments.

After a stroke, several cellular and molecular phenomena occur, including destruction of the extracellular matrix (ECM), which in turn worsens the stroke lesion. The ECM constitutes a complex environment that surrounds and supports various cells. It contains numerous signaling and structural proteins that regulate tissue homeostasis. Among these components, heparan sulfate proteoglycans (HSPGs) are known to be involved in various processes, including neurodevelopment/ neuroplasticity with the regulation of neural stem cells, and angiomodulatory mechanisms [3]. HSPGs are also known to bind and regulate the activity of several growth factors such as vascular endothelial growth factor (VEGF), transforming growth factor (TGF)-β and fibroblast growth factor-2 (FGF-2) [4]. Following a stroke, HSPGs are enzymatically degraded by an endoproteoglycanase, named heparanase, resulting in alteration of the ECM structure and reduction in the bioavailability of growth factors that normally bind to HSPGs at the lesion site [5, 6]. Therefore, degradation of HSPGs prevents the regeneration of the affected tissue. Growing evidence suggests an essential role of the ECM in brain tissue repair after an ischemic stroke. For example, the ECM was shown to be crucial for the endogenous repair response by stimulating neural and oligodendrocyte progenitor recruitment [7].

To promote the regeneration of the ECM after a lesion, a pharmacologically active molecule, i.e., the heparan sulfate mimetic (HSm) named RGTA-4131® (for ReGeneraTing Agent or HSm4131) was developed. HSm4131 is a synthetic polysaccharide that binds to extracellular structural proteins such as collagen and acts as a reservoir of growth factors [4]. Indeed, it was shown that HSm can bind different growth factors such as VEGF, FGF (-1 and -2) and TGF-β [8, 9, 10]. The molecular structure of HSm prevents its enzymatic degradation during tissue destruction and ECM remodeling [11]. In this manner, HSm protect heparin binding growth factors (HBGFs) from degradation and increase their bioavailability [12]. HBGFs, especially VEGF, are known to play an essential role in tissue repair and brain plasticity [13]. Furthermore, HSm are already used for human wound repair in several pathologies, particularly for the treatment of chronic skin wounds and corneal lesions. In the present paper, we hypothesized that HSm4131 could protect brain tissue, and promote plasticity and functional recovery after a stroke, representing a novel matrix-based therapeutic strategy.

Material and methods

Animals

All experimental procedures were approved by the regional committee on animal ethics (APAFiS#3252), and were performed at the CYCERON platform (Caen, France, agreement number: FA-118-001). Male Sprague-Dawley rats (CERJ, France) weighing 300-350g were used. Data were reported according to the ARRIVE guidelines (Animal Research: Reporting of *In Vivo* Experiments). All experiments and data analyses were performed in a blind and randomized manner.

Induction of brain ischemia

Transient cerebral ischemia was induced by intraluminal occlusion of the middle cerebral artery (MCAo) as previously described [14, 15]. Briefly, rats were anesthetized with isoflurane (2-2.5%) in a mixture of O_2/N_2O (30%/70%). During surgery, animal temperature was monitored with a rectal probe and was maintained at 37 °C with a heating blanket. A nylon filament (0.18 mm diameter) with a distal cylinder (0.39 mm diameter x 3 mm length) (Doccol, Sharon, MA, USA) was introduced into the lumen of the right external carotid, advanced through the internal carotid, and gently pushed up to the origin of the middle cerebral artery (MCA). At one hour following the occlusion, rats were re-anesthetized and the filament was withdrawn to allow reperfusion. After reperfusion, the rats were returned to their home cage after receiving analgesics (tolfedine, 10 mg/kg, i.m.) and rehydration (5 mL of saline, i.p.), which was maintained for 3 days after MCAo. Of note, the surgical procedure was associated with a 20.5% mortality in animals treated with HSm4131 or saline.

HSm4131 administration

HSm4131 (OTR3 S.A.S., Paris, France) is a 132 kDa synthetic polysaccharide, which is substituted with acetyl, carboxymethyl and sulphate groupments (Figure S1). HSm4131 or saline (0.9% NaCl) were injected (300 µL) through the tail vein. To study the therapeutic time window of HSm4131, the compound in saline was administered intravenously (1.5 mg/kg) at 1, 2.5 or 6 h after MCAo (Figure 1). To evaluate the dose response, different doses of HSm4131, i.e., 0.1 mg/kg (0.7 nmol/kg), 0.5 mg/kg (3.7 nmol/kg), 1.5 mg/kg (11.3 nmol/kg), or 5 mg/kg (37.9 nmol/kg) were similarly administered 1 h after

MCAo (Figure 1). In all other studies, HSm4131 was administered (i.v.) 1 h after MCAo at 0.5 mg/kg. The vehicle group for all these experiments received saline (300 µL, i.v.).

Measurement of physiological parameters

To examine the effect of HSm4131 administration on physiological parameters, arterial blood pressure, heart rate, blood gases and blood pH were measured in rats subjected to MCAo and treated with HSm4131 or vehicle.

MRI examinations

On day 2 and 14 following the induction of brain ischemia, each animal was anesthetized as described above and underwent magnetic resonance imaging (MRI) (7T, PharmaScan®, Bruker BioSpin, Ettlingen, Germany at the CYCERON imaging platform, Caen, France). After a scout view, T2w imaging was performed for each group with a rapid acquisition with refocused echoes (RARE) sequence (RARE factor of 8; TR/TE = 5000/16.25 ms; number of experiments (NEX) = 2; 20 contiguous slices of 0.75 mm; acquisition time = 4 min; nominal resolution = 0.15 x 0.15 x 0.75 mm^3). All MRI images were analysed with the ImageJ® software (Wayne Rasband, NIMH, Maryland, USA) [16]. Lesions on each MR image were manually delineated and the volume of infarction was corrected for edema as described by Gerriets and colleagues [17]. Animals displaying atypical lesions for the MCAo model (i.e., no cortical lesion, lesion in the hippocampus) were excluded from the study.

HSm4131 biodistribution

HSm4131 was coupled to technetium-99m (^{99m}Tc) (FRIM platform UMS34 University Paris Diderot, Paris, France) and administered at 0.5 mg/kg (i.v.) immediately after reperfusion, (i.e. 1 h after MCAo). Animals were euthanized at different time points: 5 min, 1, and 3 h following HSm4131-^{99m}Tc administration. After washing the vascular compartment through transcardiac perfusion of saline, radioactivity was measured in each hemisphere using a gamma counter.

Behavioral tests

Neurological score

The neurological score was performed following 14 items based on the modified version of the method described by Bederson and colleagues [18]. A maximal score of 28 indicated normal sensorimotor response [19]. Each item was scored as 0 (severe deficit), 1 (minor deficit), or 2 (no deficit).

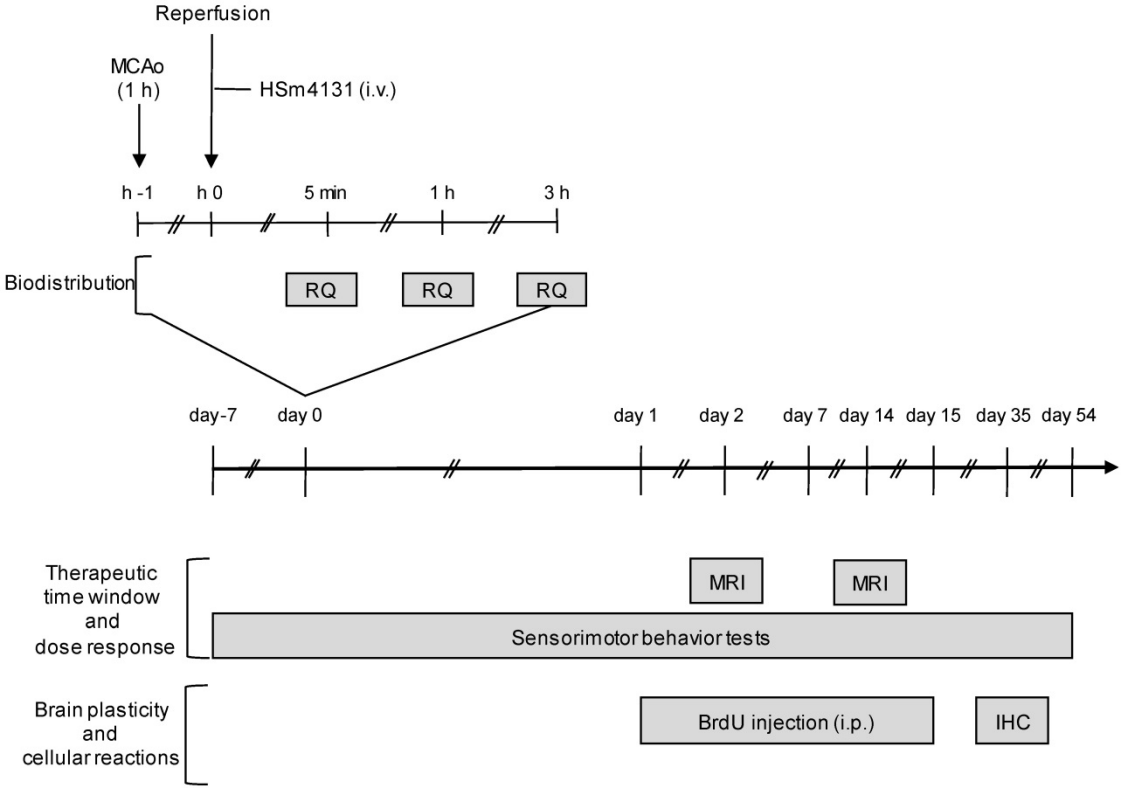

Figure 1: Experimental protocols. Depicted is the experimental protocol to evaluate the therapeutic time window, the dose response of HSm4131, the brain plasticity induced by HSm4131, and the biodistribution of HSm4131-^{99m}Tc after MCAo. BrdU: Bromodeoxyuridine; IHC: Immunohistochemistry; MCAo: middle cerebral artery occlusion; MRI: magnetic resonance imaging; RQ: radioactivity quantification.

Limb placing test

The limb placing test was performed as described by De Ryck and colleagues [20]. Each item was scored as 0 (major deficit), 1 (minor deficit), or 2 (no deficit). The maximal score obtained with a healthy rat was 24 [19].

Corner test

The corner test was performed as described by Schallert and collaborators [21] to evaluate the sensorimotor and postural asymmetries. The rearing and reversing in either direction (ipsilateral or contralateral to the ischemic lesion) after the corner exploration were noted. The test was repeated 10 times every 2 min. The index of lateralization (LI) was calculated according to Haelewyn and collaborators [22].

Cylinder or limb-use asymmetry test

To assess forelimb use asymmetry, the use of the ipsilateral, contralateral or bilateral forelimbs to explore the cylinder was noted for 20 times according to Schallert and collaborators [23].

Adhesive removal test

The adhesive removal test was employed to assess somatosensory deficits and motor coordination [24]. Animals were placed in a transparent Plexiglass box (20×25×32 cm) after a habituation period of 60 s; two adhesive tapes (1×1 cm) were randomly applied with equal pressure on each forepaw. The time spent to detect and remove the adhesive was measured (maximum: 120 s).

Reverse transcription and real-time quantitative PCR

Total RNA from cells or tissues was extracted and purified using RNeasy Micro Kit (Qiagen, Courtaboeuf, France). RNA concentration was measured with the NanoDrop™ 2000 spectrophotometer (Thermo Fisher Scientific, USA) and reverse transcribed into complementary DNA (cDNA) with AMV® reverse transcriptase (Promega). PCR amplification and analysis were achieved using the Applied Biosystems QuantStudio™ 6 & 7 Flex Real-Time PCR System (Thermo Fisher Scientific, USA). Amplification reactions were performed using Takyon™ Low Rox SYBR® MasterMix dTTP Blue (Eurogentec, Belgium) with primers designed and purchased from Eurogentec, Belgium (Table S1). Cyclophin-A was used as an endogenous RNA control (housekeeping gene). Samples were run in triplicates and amplification cycles were as follows: an activation stage at 95 °C for 3 min, followed by 40 cycles at 95 °C for 3 s and 60 °C for 30 s. The expression level was calculated using the comparative Ct method ($2^{-\Delta Ct}$) after normalization to the housekeeping gene (Cyclophilin-A).

Immunohistochemistry

Rats were injected with BrdU (50 mg/kg, i.p.) from day 1 to day 15 post-MCAo and were euthanized at day 35. Briefly, under deep anesthesia with 5% isoflurane in a mixture of O_2/N_2O (30%/70%), animals underwent a transcardiac perfusion of a heparinized saline (10 IU/mL) followed by a 4% paraformaldehyde (PFA) perfusion (Sigma, France). Brains were then placed in 4% PFA for 48 h and put into a solution of phosphate-buffered saline (PBS) with 30% sucrose. Cryosections (50 µm) were obtained in the coronal plane using a microtome (HM 450 Sliding Microtome, Thermo Scientific™).

To assess neurogenesis, sections were incubated with the immature neuronal marker doublecortin (DCX) (polyclonal rabbit anti-DCX, Abcam 0.3 µg/mL) or the mature neural marker NeuN (polyclonal rabbit anti-NeuN, Abcam 1.5 µg/mL) along with the proliferation marker BrdU (polyclonal rat anti-BrdU, Roche 0.2 µg/mL).

To analyze angiogenesis, the rat endothelial cell antigen marker (RECA-1) (monoclonal mouse anti-RECA-1, AbD Serotec 5 µg/mL) was used along with the proliferation cell marker Ki67 (rabbit polyclonal anti-Ki67 antibody, Abcam 5 µg/mL). Thus, cells positive for RECA-1 and Ki-67 correspond to proliferating endothelial cells, an indicator of angiogenesis. Glial and inflammatory reactions were assessed with the astrocytic marker glial fibrillary acidic protein (polyclonal rabbit anti-GFAP, DAKO 5.8 µg/mL) and the CD68 marker (polyclonal mouse anti-CD68, Abcam 2 µg/mL), respectively.

Briefly, the sections were washed in PBS solution and blocked with a solution of PBS containing 3% bovine serum albumin (BSA) (Sigma) and 0.1% Triton (Sigma), before overnight incubation with the primary antibody in PBS with BSA (1%) and Triton (0.1%) at 4 °C. Sections were washed again with PBS followed by 2 h incubation with the appropriate secondary antibodies (Alexa Fluor® 555, 488, 4 µg/mL, Invitrogen) and the nuclear marker, Hoechst 33342 (1/500, Sigma Aldrich) at room temperature. Sections were washed with PBS and placed on a slide before the application of the coverslip.

After image acquisition with a microscope (Leica microsystems DMi8), all images were analyzed with the ImageJ® software (Wayne Rasband, NIMH, Maryland, USA) [17]. DCX, GFAP and CD68 were quantified by measuring the pixels in the ipsilateral (ischemic) hemisphere, which showed statistically significant higher intensity than the control

homologous area in the contralateral (non-ischemic) hemisphere ($p < 0.001$; Student's t- test distribution table (mean + 3.291*SD). Angiogenesis was quantified by counting the RECA-1$^+$/Ki-67$^+$ double positive cells and expressing the results as the percentage of Ki-67$^+$ cells.

To study the ECM heparan sulfate (HS) distribution following MCAo, tissue cryosections (50 µm) were washed and incubated for 2 min with 50 mM NH_4Cl in PBS and washed again. Sections were then blocked with 3% BSA/PBS for 1 h. HS were then stained with an antibody that recognizes the 10E4 epitope present in many HS (1:100), and a donkey anti-mouse secondary antibody conjugated to the Alexa-488 fluoroprobe (Molecular Probes, 1:200). Tissue sections were then incubated with DAPI (1 µg/mL) for 5 min and rinsed. To further confirm the specificity of the staining, tissues were treated with a heparitinase cocktail (heparitinase I/II/III 2/0.2/0.2 U/mL) for 6 h at room temperature, followed by washes before HS staining. Images were obtained using a spinning disk inverted confocal microscope (IX81 DSU Olympus, 60 N.A. 1.35) coupled to an Orca Hamamatsu RCCD camera (Olympus®). Image processing and analysis were done using the ImageJ® software (Wayne Rasband, NIMH, Maryland, USA) [16].

Statistical analyses

Data were analyzed by the two-tailed Student's t-test or analysis of variance (one or two-way ANOVA) followed by the Dunnett's or Tukey HSD tests (JMP® program, SAS Institute, Cary, NC, USA) when appropriate. Data were expressed as mean ± standard deviation (SD) or median ± interquartile range (IQR). In all analyses, statistical significance was set at a p-value < 0.05.

Results

The HS mimetic is neuroprotective

In initial experiments, HSm4131 at 1.5 mg/kg was administered (i.v.) 1 h after the stroke onset, which resulted in the reduction of the lesion volume by up to 30% compared to the vehicle (Student's t-test; $p < 0.05$) (Figure 2A). In these experiments, the volume reduction was still observed on day 14 after the stroke (Student's t-test; $p < 0.05$) (Figure 2A).

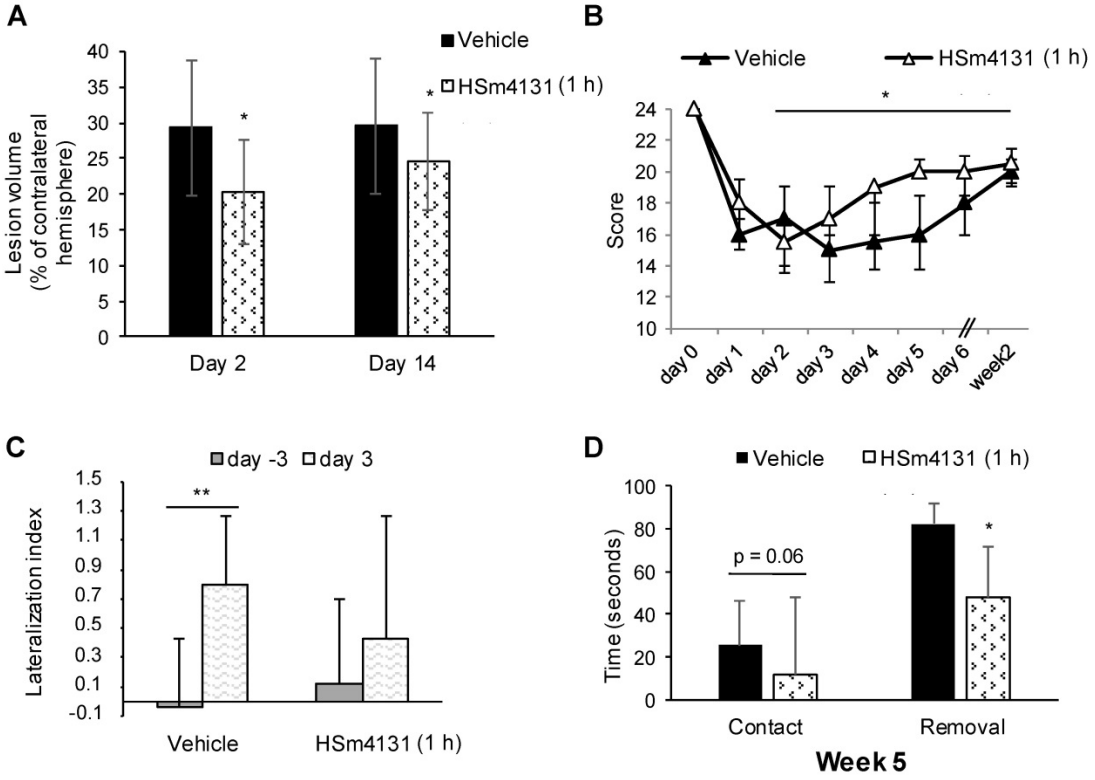

Figure 2: Effect of HSm4131 on the lesion volume and functional recovery. (A) HSm4131-induced neuroprotective effects after MCAo (vehicle n = 12; HSm4131 n = 7) on day 2 and 14 post-MCAo (*Student's t-test; $p < 0.05$); **(B)** Limb placing test (median ± IQR) (vehicle n = 7-9; HSm4131 n = 5-9). *Day 14 different from day 2 in the HSm4131-treated group (one-way ANOVA followed by a post-hoc Tukey HSD test; $p < 0.05$); **(C)** Lateralization index (LI) evaluated with the corner test at day -3 and day +3 (mean ± SD) (**one-way ANOVA followed by a post-hoc Dunnett's test; $p < 0.01$); **(D)** Assessment of motor coordination with the adhesive removal test on week 5 post-MCAo. The HSm4131-treated group removed the adhesive on the contralateral forepaw faster than the vehicle group (mean ± SD) (vehicle n = 8; 1.5 mg/kg HSm4131 n = 8) (*Student's t-test; $p < 0.05$).

Sensorimotor deficits were evaluated in these animals using the limb placing and corner tests. The HSm4131-treated group showed a significantly faster recovery between day 2 and week 2 post-MCAo compared to the vehicle group (one-way ANOVA followed by Tukey HSD test; $p < 0.05$) (Figure 2B). Administration of HSm4131 prevented brain lateralization, as shown by the corner test (one-way ANOVA followed by Dunnett's test; $p < 0.05$) (Figure 2C). Functional recovery during the chronic stage was assessed using the adhesive removal test. HSm4131-treated animals removed the adhesive on the contralateral side faster than the control animals (Student's t-test; $p < 0.05$), demonstrating better sensorimotor recovery 5 weeks after ischemia (Figure 2D).

Therapeutic time window

To determine the therapeutic time window of HSm4131, we administered the compound 1, 2.5 or 6 h post-MCAo. As shown above (Figure 2A), HSm4131 (1.5 mg/kg) was effective in reducing infarction volume when administered at 1 h post-MCAo (Figure 3A). Quantification of the lesion volume by MRI confirmed a significant 30% reduction of the lesion volume on day 2 post-MCAo when HSm4131 was administered 1 h after MCAo, while HSm4131 had no significant effect when administered 2.5 or 6 h after stroke induction (one-way ANOVA followed by Tukey HSD test; $p < 0.05$) (Figure 3A and 3B). In these experiments, there was no significant difference by one way ANOVA between the vehicle- and HSm4131-treated groups on day 14 post-MCAo ($p = 0.08$) (Figure 3A and 3C).

These data indicate that administering HSm4131 1 h after ischemia is the optimal time window that confers the best neuroprotection. Thus, this time of administration was used for the following studies.

Optimal dose of HSm4131

In order to determine the optimal neuroprotective dose of HSm4131, we tested 4 doses of the compound, i.e., 0.1, 0.5, 1.5, and 5 mg/kg. HSm4131, administered at 0.5 and 1.5 mg/kg, induced a significant reduction of the lesion volume when quantified 2 days after the induction of ischemia (one-way ANOVA followed by Tukey HSD test; $p < 0.001$) (Figure 4A, 4B). However, 0.5 mg/kg of HSm4131 conferred greater neuroprotection to the treated animals, with a reduction of the lesion volume of up to 42% compared to the vehicle group (one-way ANOVA followed by a Tukey HSD test; $p < 0.001$) (Figure 4A and 4B). Significantly, the neuroprotective effect for the 0.5 mg/kg dose was maintained on day 14 after the stroke (one-way ANOVA followed by Tukey HSD test, $p < 0.05$) (Figure 4A and 4C).

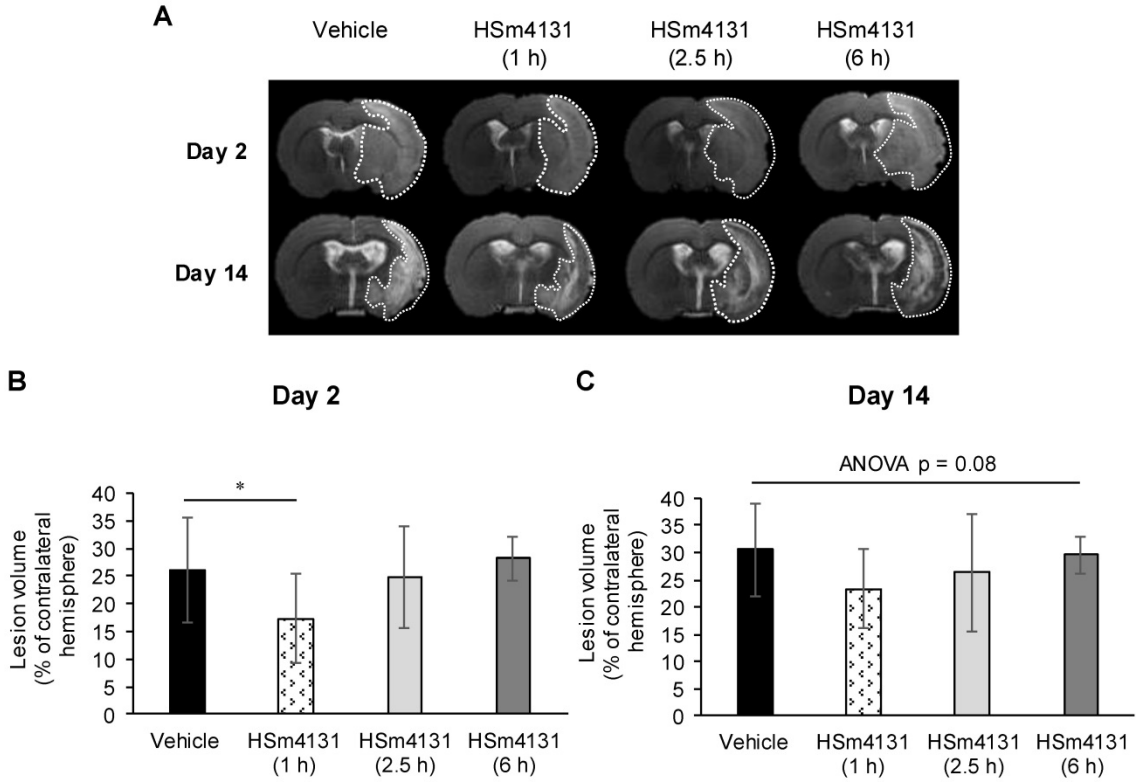

Figure 3: Therapeutic time window of HSm4131. (A) Representative MRI on day 2 and 14 post-MCAo; **(B)** Infarct volumes on day 2 and **(C)** day 14 (mean ± SD) (vehicle n = 21; 1.5 mg/kg HSm4131 (1 h n = 15; 2.5 h n = 10, and 6 h n = 6)) (*one-way ANOVA followed by a post-hoc Tukey HSD test, $p < 0.05$).

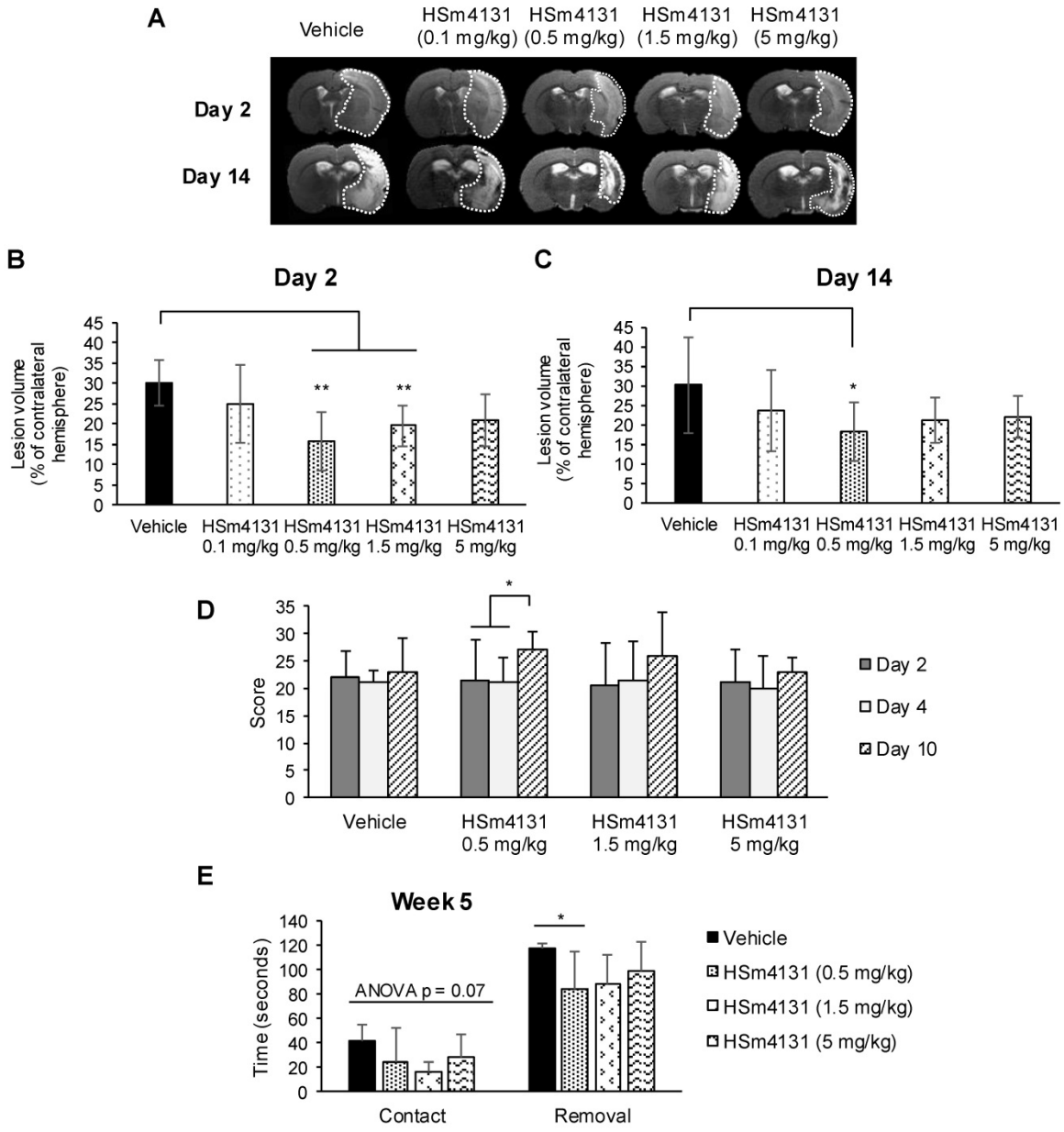

Figure 4: HSm4131 dose response after MCAo. Representative MRI of the lesions on day 2 and 14 (n = 7-11); **(B)** Infarct volumes on day 2 (mean ± SD) (vehicle n = 11; HSm4131 (0.1 mg/kg n = 7; 0.5 mg/kg n = 10; 1.5 mg/kg n = 10; 5 mg/kg n = 7)) (**One-way ANOVA followed by a post-hoc Tukey HSD test, $p < 0.01$); **(C)** Infarct volumes on day 14 (mean ± SD) (vehicle n = 11; HSm4131 (0.5 mg/kg n = 10; 1.5 mg/kg n = 10; 5 mg/kg n = 7)) (*one-way ANOVA followed by post-hoc Tukey HSD test, $p < 0.05$); **(D)** Evolution of the neurological score. The maximal score for normal responses is 28; (median ± IQR) (vehicle n = 8; HSm4131 (0.5 mg/kg n = 10; 1.5 mg/kg n = 10; 5 mg/kg n = 7)) (*one-way ANOVA followed by a post-hoc Tukey HSD test, $p < 0.05$); **(E)** Adhesive removal test on week 5 post MCAo. The times to detect (contact) and to remove (removal) the adhesive on the contralateral side were measured in seconds (Mean ± SD) (vehicle n = 8; HSm4131 (0.5 mg/kg n = 10; 1.5 mg/kg n = 10; 5 mg/kg n = 7)) (*one-way ANOVA followed by a post-hoc Tukey HSD test, $p < 0.05$).

The assessment of sensorimotor deficits using the neurological score demonstrated greater recovery for the animals treated with 0.5 mg/kg HSm4131 on day 10 compared to day 2 and 4 (one-way ANOVA followed by Tukey HSD test; $p < 0.05$), whereas vehicle animals showed no significant improvement during the test period (Figure 4D). Sensorimotor recovery persisted for at least 5 weeks after ischemia in the animal group treated with 0.5 mg/kg HSm4131. No significant statistical difference was observed between vehicle- and HSm4131-treated animals for the time to detect the adhesive tape (one-way ANOVA; $p = 0.07$). More importantly, only animals treated with 0.5 mg/kg HSm4131 removed the adhesive tape on the contralateral side significantly faster than the vehicle group (one-way ANOVA followed by Tukey HSD test; $p < 0.05$) (Figure 4E).

Collectively, these results demonstrate that HSm4131 administered 1 h following stroke at the dose of 0.5 mg/kg confers the best neuroprotection and recovery. Therefore, this dose and timing were used for the following studies.

HSm4131 does not alter physiological parameters

Physiological parameters were continuously monitored from 30 min before MCAo up to 1 h after reperfusion. Blood pressure, pH, $paCO_2$, paO_2, and body temperature did not show any significant variation following HSm4131 administration (Table 1). Moreover, no significant difference was found between the treated and vehicle groups (two-way ANOVA; $p > 0.05$) before and after HSm4131 administration.

Table 1: Assessment of physiological parameters.

		Pre-MCAo	1 h MCAo	Post-MCAo
Arterial pressure (mmHg)	Vehicle	87 ± 14	81 ± 12	74 ± 10
	HSm4131	91 ± 8	81 ± 7	73 ± 4
Heart rate (bpm)	Vehicle	361 ± 50	366 ± 51	372± 46
	HSm4131	407 ± 16	405 ± 33	407 ± 42
pH	Vehicle	7.43 ± 0.08	7.40 ± 0.14	7.39 ± 0.02
	HSm4131	7.50 ± 0.04	7.44 ± 0.02	7.43 ± 0.02
$paCO_2$ (mmHg)	Vehicle	40.9 ± 7.4	42.9 ± 12.6	44.8 ± 15.4
	HSm4131	36.1 ± 3.9	42.2 ± 5.9	42.5 ± 5.6
paO_2 (mmHg)	Vehicle	151.8 ± 39.5	144.6 ± 39.5	135.3 ± 38.8
	HSm4131	149.8 ± 32.3	132.2 ± 21.3	120.0 ± 16.8
Hct	Vehicle	44.3 ± 1.8	44.4 ± 2.1	43.2 ± 2.4
	HSm4131	44.5 ± 0.7	43.5 ± 0.5	42.7 ± 1.1
Temperature (°C)	Vehicle	37.6 ± 0.3	38.0 ± 0.2	37.9 ± 0.2
	HSm4131	37.7 ± 0.3	37.9 ± 0.1	37.9 ± 0.1

Assessment of blood pressure, pH, CO_2 pressure, O_2 pressure, and body temperature 30 min before MCAo, 1 h after MCAo and 1 h after reperfusion (mean ± SD) (vehicle n = 6; 0.5 mg/kg HSm4131 n = 4).

Distribution of HSm4131-Tc^{99m} in brain

Animals treated intravenously with HSm4131-Tc^{99m} showed a significant increase of the radioactivity in the ipsilateral hemisphere between 5 min and 1 h following MCAo (Figure 5). Moreover, no significant difference in the amount of radioactivity was detected between 1 h and 3 h in the ipsilateral hemisphere. Furthermore, the radioactivity count was significantly higher in the ipsilateral hemisphere compared to the contralateral hemisphere 1 h following MCAo (two-way ANOVA followed by a post-hoc Tukey HSD test; $p < 0.05$) (Figure 5).

HSm4131 restores HS distribution

HS distribution was analyzed 35 days after MCAo by immunohistochemistry using the HS marker, 10E4. HS staining was markedly altered following stroke in vehicle animals, compared to healthy animals (Figure 6A and 6B). Nonetheless, in the ipsilateral hemisphere, along the ischemic boundary zone, the tissue displayed higher cell density and better matrix structure in animals treated with HSm4131 compared to vehicle animals (Figure 6B). Treatment of the brain slices with heparitinases demonstrated the specificity of the HS staining (Figure 6C).

HSm4131 improves brain plasticity

HSm4131 enhances angiogenic factor gene expression

Gene expression of the well-known angiogenic factors, VEGF-A and Ang-2, also known as neurogenic factors [25][26][27], was analyzed on day 14 after MCAo. Both VEGF-A and Ang-2 gene expression increased in the ipsilateral hemisphere in animals treated with HSm4131 compared to healthy animals or those treated with saline (one-way ANOVA followed by post-hoc Tukey HSD test; $p < 0.05$) (Figure 7). These results suggest that HSm4131 treatment could improve post-ischemic brain plasticity such as angiogenesis and neurogenesis.

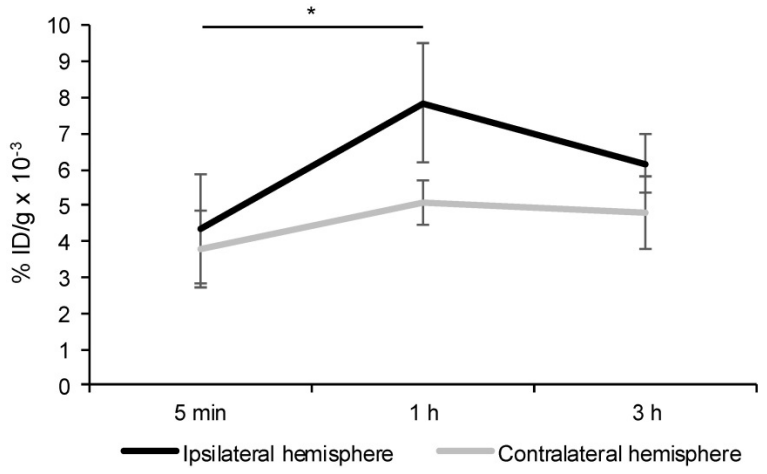

Figure 5: Biodistribution of HSm4131-^{99m}Tc in the ipsilateral and contralateral hemispheres. Percentage of HSm4131-^{99m}Tc radioactivity per gram of tissue (% ID/g) in the ipsilateral and the contralateral hemispheres. HSm4131-^{99m}Tc was administered at a dose of 0.5 mg/kg immediately following reperfusion, which was performed after 1 h of MCAo. Radioactivity of HSm4131-^{99m}Tc in the brain tissue was quantified at 5 min (n = 6), 1 h (n = 6) and 3 h (n = 6) in the ipsilateral hemisphere, and at 5 min (n = 6), 1 h (n = 6) and 3 h (n = 7) in the contralateral hemisphere after reperfusion following a 1 h MCAo (mean ± SD). *1 h different from 5 min in the ipsilateral hemisphere, and from 1 h in the contralateral hemisphere (Two-way ANOVA (hemisphere $p < 0.001$; time $p < 0.001$; hemisphere * time $p = 0.04$) followed by a post-hoc Tukey HSD test, $p < 0.05$).

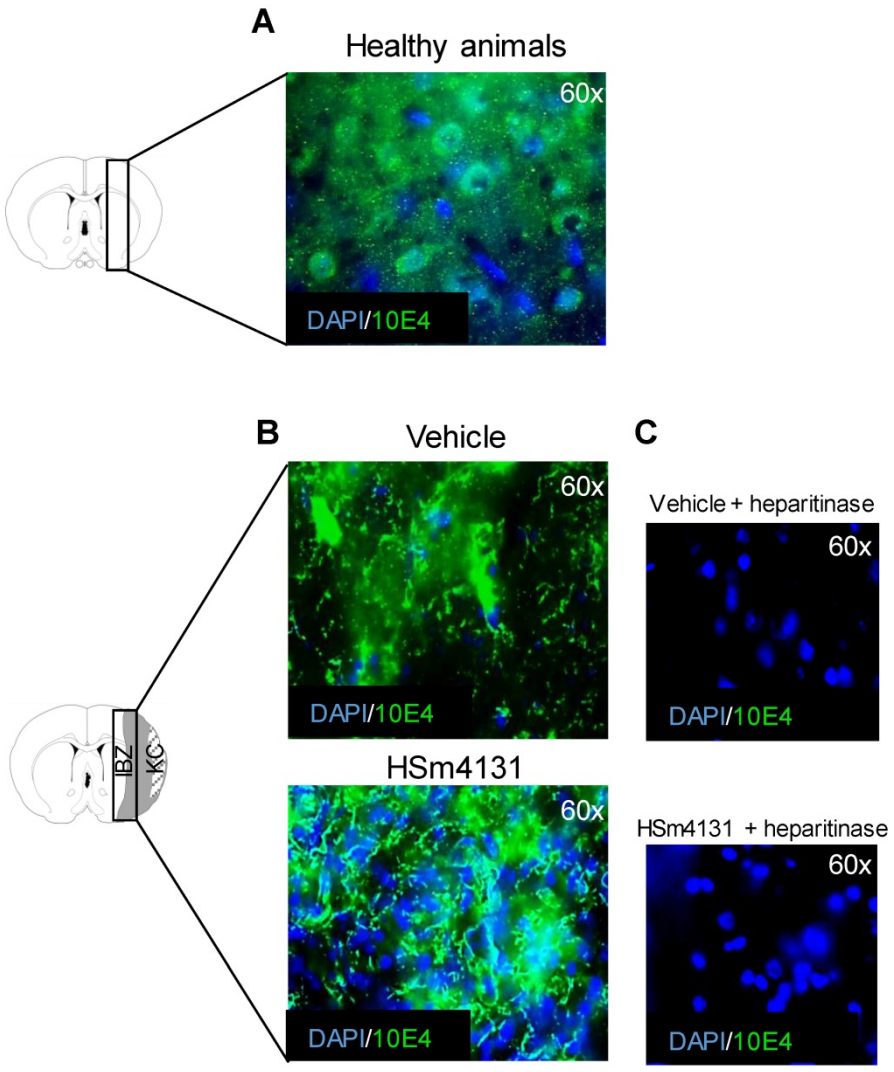

Figure 6: Analysis of post-ischemic HS distribution. (A) Representative images of HS distribution (green) in healthy animals; **(B)** Representative images of HS distribution in the ipsilateral hemisphere in the vehicle and HSm4131-treated groups (vehicle n = 9; 0.5 mg/kg HSm4131 n = 6); **(C)** Representative slices illustrating the complete disappearance of the green staining following the treatment with heparitinase.

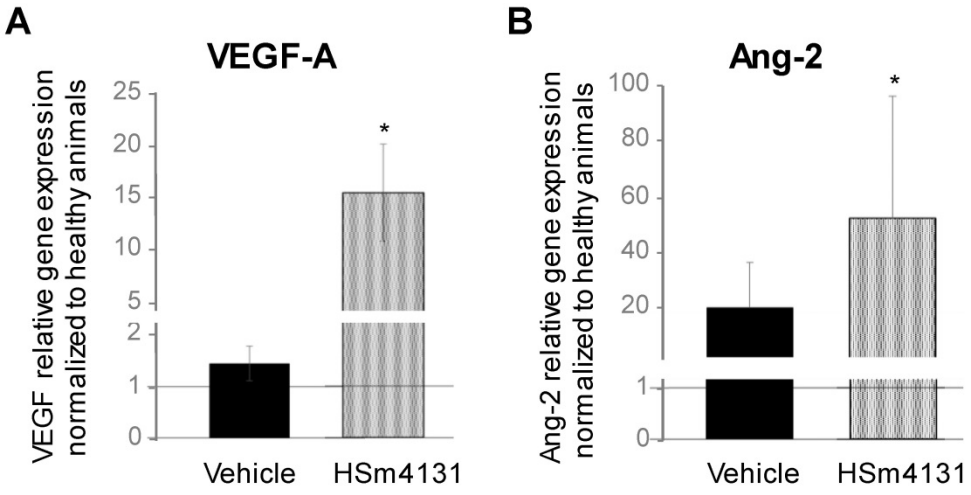

Figure 7: Effect of HSm4131 on gene expression of angiogenic factors. (A) VEGF-A and **(B)** Ang-2 gene expression on day 14 after MCAo in the ipsilateral hemisphere. Results are expressed as relative gene expression to the cyclophilin-A housekeeping gene normalized to healthy animals (mean ± SD) (healthy animals n = 5; vehicle n = 3; 0.5 mg/kg HSm4131 n = 3) (*one-way ANOVA followed by a post-hoc Tukey HSD test, $p < 0.05$).

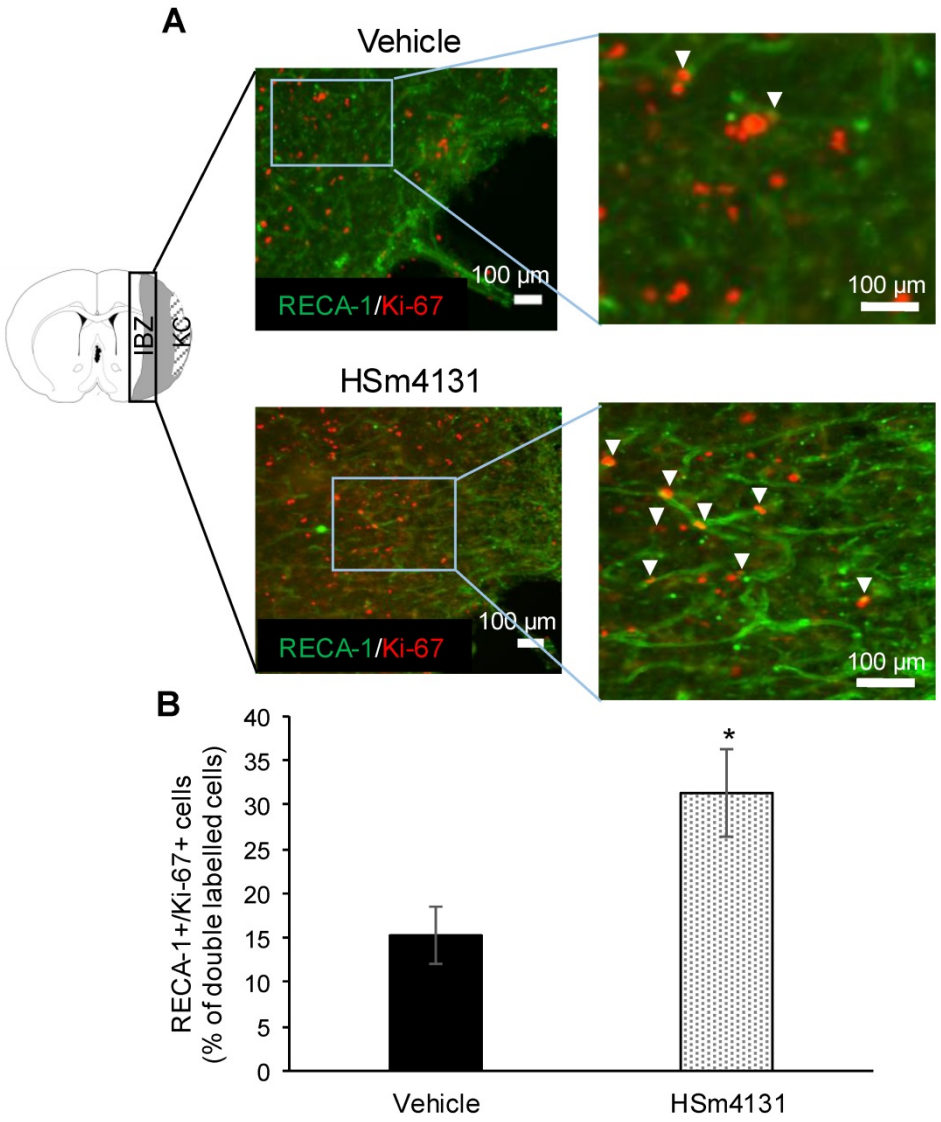

Figure 8: Analysis of post-ischemic angiogenesis. (A) Representative images of RECA-1+ (endothelial cell antigen marker)/Ki-67+ (proliferative cell marker) double positive cells marked by white arrowheads; **(B)** Number of RECA-1+/Ki-67+ cells expressed as the percentage of Ki-67+ cells in the peri-infarct area (mean ± SD) (vehicle n = 4; 0.5 mg/kg HSm4131 n = 4). *Student's t-test; $p < 0.05$. KC: Kystic cavity; IBZ: Infarct boundary zone.

HSm4131 enhances post-ischemic angiogenesis

Post-ischemic angiogenesis was quantified 35 days after MCAo by counting the RECA-1/Ki-67 double positive cells in the peri-infarct regions and expressed as the percentage of Ki-67 positive cells. The number of RECA-1/Ki-67 double positive cells was significantly higher in animals treated with HSm4131 compared to the vehicle group (Student's t-test; $p < 0.05$) (Figure 8).

HSm4131 enhances post-ischemic neurogenesis

Post-ischemic neurogenesis was quantified in the ipsilateral hemisphere 35 days after MCAo by quantifying immature neurons using the marker, DCX, and mature neurons using BrdU/NeuN double-positive cells. The DCX staining area in the sub-ventricular zone (SVZ) and around the lateral ventricle (LV) increased in animals treated with HSm4131 compared to the vehicle group (Student's t-test; $p < 0.05$) (Figure 9A). Similarly, the number of BrdU/NeuN double positive cells in the ipsilateral (ischemic) hemisphere increased in animals treated with HSm4131 compared to vehicle animals (Student's t-test; $p < 0.05$) (Figure 9B).

HSm4131 does not modify astroglial and immune reactions

The astroglial and immune reactions in the ipsilateral hemisphere assessed by GFAP and CD68 immunostaining were not significantly different between vehicle and treated animals 35 days post-MCAo (Figures S2 and S3).

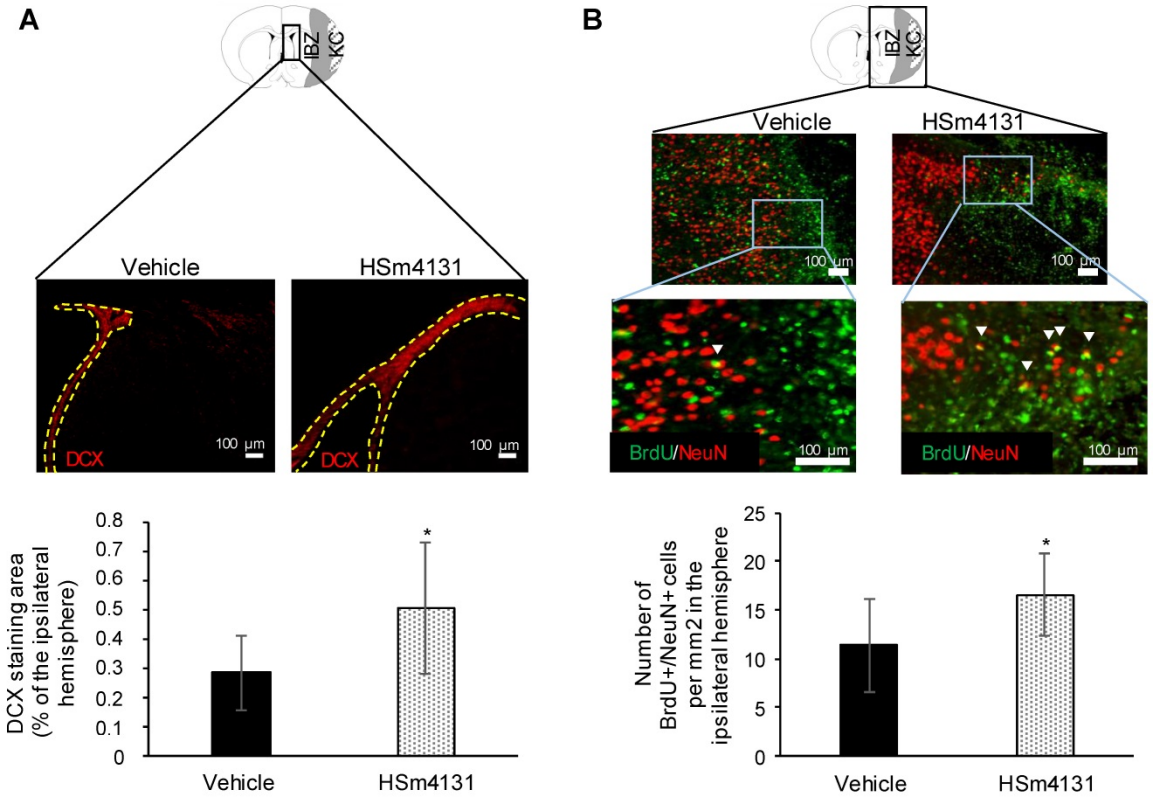

Figure 9: Analysis of post-ischemic neurogenesis. (A) Representative images of DCX$^+$ cells and corresponding area of DCX staining measured around the lateral ventricle expressed as the percentage of the ipsilateral hemisphere (mean ± SD) (vehicle n = 9; 0.5 mg/kg HSm4131 n = 7); **(B)** Representative images of BrdU$^+$ (green)/NeuN$^+$ (red) cells (indicated by white arrow heads) and the number of BrdU$^+$/NeuN$^+$ cells per mm^2 in the ipsilateral hemisphere (mean ± SD) (vehicle n = 9; 0.5 mg/kg HSm4131 n = 6). *Student's t-test, $p < 0.05$. KC: Kystic cavity; IBZ: Infarct boundary zone.

Discussion

In the present study, we have shown that a cellular matrix-based therapy using HSm4131 provides long-lasting neuroprotection. This was indicated by improved functional recovery as well as increase in neurogenesis and angiogenesis.

Significant reduction of the infarct volume was observed 2 days after brain ischemia in animals treated with intravenous administration of HSm4131 for 1 h. More importantly, this treatment also resulted in improved sensorimotor recovery, highlighting the clinical translational potential of HSm4131 treatment. Based on the dose response effect of HSm4131, administration of 0.5 mg/kg HSm4131 confers the best long-lasting neuroprotective effect, both during the acute (2 days) and chronic (14 days) phases after brain ischemia, and significant functional recovery. These results are in accordance with those by Hill and colleagues [28] showing that treatment with an HSPG improves functional recovery assessed by neurological scoring and cylinder test after MCAo for 1 h in rats.

The benefits incurred by HSm4131 could be explained by its high sulfation index, which allows its binding to HBGFs, and its resistance to enzymatic degradation, thereby enhancing HBGF bioavailability. Interestingly, fewer benefits were observed when using a higher dose of HSm4131, which could be explained by the wash-out theory; HSm4131 in excess and bound to HBGFs may be eliminated by the blood circulation, resulting in a narrow bell shaped dose-dependent effect, as previously described with a compound comparable to HSm4131 that was used to stimulate muscle regeneration after total crushing [29]. Moreover, HSm bind to several growth factors, potentiating their activity [8], and some of them have been shown to worsen the ischemic lesion during the acute phase of stroke [30]. Thus, excess HSm may lead to potentiation of the deleterious effect of these growth factors, thereby reducing the neuroprotective effect of HSm.

To elucidate the mechanism underlying HSm4131-induced neuroprotection, regeneration and functional recovery after ischemic stroke, we analyzed the biodistribution of HSm4131 in the affected hemisphere, and its effects on physiological parameters as well as on some indices of brain plasticity, namely angiogenesis and neurogenesis. HSm4131 did not alter any of the physiological parameters following intravenous administration. Moreover, the analysis of HSm4131-^{99m}Tc

biodistribution showed a significant and persistent increase in the accumulation of the compound in the ipsilateral (ischemic) hemisphere following MCAo. However, as the basal lamina contains abundant heparin-binding proteins, additional studies will be needed to definitely assess the penetration of HSm4131 into the brain parenchyma.

To understand how HSm4131 provides beneficial effects after ischemic stroke, we analyzed HS distribution by immunohistochemistry. Improved matrix organization and higher cell density were observed in the ischemic hemisphere when animals were treated with HSm4131. This result supports previous findings showing that HSm protect or restore the ECM, and protect growth factors, leading to tissue regeneration and cell proliferation [4]. Based on these results, one might hypothesize that HSm4131 neuroprotection may be due to an indirect effect following ECM protection and/or reparation. Additional studies will be needed to determine the direct and indirect mechanisms by which HSm4131 protects the brain from ischemia-induced damage and favors functional recovery.

As HSm have been shown to protect some well-known angiogenic and neurogenic factors such as VEGF [8], we investigated the effects of HSm4131 on post-ischemic brain cellular reactions, including angiogenesis and neurogenesis. First, we showed that HSm4131 enhanced VEGF-A and Ang-2 gene expression 14 days after MCAo, supporting its beneficial effect on post-ischemic brain plasticity. Both VEGF-A and Ang-2 have been previously shown to enhance angiogenesis and neurogenesis [25, 26, 27] . However, our studies only showed enhanced gene expression, and did not assess protein expression. Nevertheless, HSm4131 enhanced angiogenesis in the peri-infarct region, as shown by immunohistochemistry. These results are in accordance with the study by Desgranges and colleagues [31] which reported that an heparan-like molecule could improve neovascularization. Similarly, Rouet and colleagues [8] have shown that another HSm modulated angiogenesis by interacting with VEGF. Therefore, one might speculate that the HSm4131 effects on post-ischemic angiogenesis may be mediated through the potentiation of VEGF activity in the ischemic brain hemisphere.

Likewise, post-ischemic neurogenesis was found to be higher in the animal group treated with HSm4131 compared to the vehicle group. Neurogenesis is well known to occur after ischemic stroke [32, 33]. However, the exact role of the ECM in this phenomenon is still not well established. HSPGs are thought to affect proliferation, differentiation and maintenance of stem-cell niches [34], which could explain the significant increase in the generation of immature and mature neurons in animals treated with HSm4131. Moreover, this effect could also be due to the interaction of HSm4131 with FGF2 and/or VEGF, which are known to be involved in post-ischemic neurogenesis [35, 36]. Indeed, VEGF has a key role in post-stroke recovery as it promotes both angiogenesis and neurogenesis *in vivo* following ischemic stroke [25]. Nonetheless, further analyses will be needed to establish whether HSm4131 acts directly on neurogenesis or indirectly through its reduction of ischemic brain damage.

As HSm4131 induces neuroprotection and improves functional recovery during the acute and chronic phases after a stroke, we hypothesized that it could also act on post-ischemic inflammation and gliosis. Immune and glial reactions were therefore evaluated by CD68 and GFAP staining, respectively. Innate immune inflammation has been shown to play a role in tissue repair and remodeling during the chronic phase after a stroke [37]. Suppressing inflammation and microglial activation stimulates the accumulation of new neurons in the injured striatum following ischemic stroke in adult rats [38]. HSPGs and an HS mimetic analogue of HSm4131 were shown to bind chemokines of the TGF-β family [39][40], which are anti-inflammatory chemokines that suppress macrophage cytokine production [41]. However, other studies have shown that inflammation could participate in the regeneration of the central nervous system by clearing cell debris and secreting multiple growth factors [42]. Our analysis of the $CD68^+$ monocyte lineage population showed no significant difference between the HSm4131- and vehicle-treated groups. Considering the complexity of the inflammatory reaction, HSm4131 could have specific effects on distinct cells (macrophages/microglia, neutrophils or other leukocytes). Indeed, in a periodontitis model, an HSm analogue of HSm4131 has been shown to reduce inflammation by decreasing polymorphonuclear leukocyte migration to the lesion site [43]. Moreover, following stroke, brain tissue inflammation is the highest within the first 24 hours following brain ischemia [44], while in our study, inflammation was evaluated 35 days following stroke onset, which could have been too late to detect a difference in $CD68^+$ cells.

Quantification of GFAP staining showed no significant difference between HSm4131- and vehicle-treated groups. Many studies have reported that a decrease in gliosis is associated with the reduction of the infarct size [45]. Despite this association, the exact role of astrocytes during stroke is still under extensive investigation. Previous studies have shown that glial scar formation prevents the

overwhelming inflammatory response, limits cellular degeneration, and protects healthy tissue from uncontrolled tissue damage [46, 47]. Therefore, further investigation needs to be conducted to determine the exact role of HSPGs and HSm in immune reactions and gliosis following ischemic stroke. Our study focused on the immune and glial reactions in the ipsilateral hemisphere. Further investigation is needed to better understand the effects of HSm4131 on these reactions by analyzing immune cell populations in specific brains regions and from serum samples at different time points.

Conclusion

This study explores for the first time the potential of HSm4131 as a neuroprotective therapy for ischemic stroke in a rat model. HSm4131 shows promising beneficial effects after stroke, an effect that is quite encouraging given the current lack of treatment and the narrow therapeutic window of t-PA. HSm have proven their efficacy in tissue repair in many pathologies, including tendon injuries, ischemic muscles, periodontitis, inflammatory diseases, and bone defects [40]. More importantly, the regenerative effects of HSm have been observed in more than 20,000 patients with chronic skin wounds and 5,000 patients with corneal ulcers without any reported side effects [40]. Based on the improvement of functional recovery and brain plasticity in the acute and chronic phases of stroke, this study reveals the potential of HSm4131 as a promising treatment for ischemic stroke.

Abbreviations

Ang-2: angiopoetin-2; GFAP: astrocytic marker glial fibrillary acidic protein; BSA: bovine serum albumin; DCX: doublecortin; ECM: extracellular matrix; FGF-2: fibroblast growth factor-2; HSPGs: heparan sulfate proteoglycans; HSm: heparan sulfate mimetic; HBGFs: heparin binding growth factors; LV: lateral ventricle; MRI: magnetic resonance imaging; MCA: middle cerebral artery; MCAo: middle cerebral artery occlusion; NEX: number of experiments; MCAo: occlusion of the middle cerebral artery; PFA: paraformaldehyde; PBS: phosphate-buffered saline; RARE: rapid acquisition with refocused echoes; RECA-1: rat endothelial cell antigen marker-1; rt-PA: recombinant tissue plasminogen activator; RGTA®: Regenerating agent; SVZ: sub-ventricular zone; Tc^{99m}: technetium-99m; TGF-β: transforming growth factor-β; VEGF: vascular endothelial growth factor.

Acknowledgements

This work was supported by CNRS, the Ministère de l'Enseignement Supérieure et de la Recherche, the Université de Caen Normandie, OTR3 S.A.S, the ANR (Agence Nationale de la Recherche, ANR-15-CE18-0029-01- « MAESTRO »), and the Conseil Régional de Normandie. The authors wish to also thank the FRC (Fédération de la Recherche pour le Cerveau) and the site smart.servier.fr for their image bank, which was used for the graphical abstract illustration. The authors thank Dr. Martine Torres for her critical reading of the manuscript and editorial assistance.

Supplementary Material

Supplementary figures and tables.
http://www.thno.org/v08p5814s1.pdf

Competing interests

This study was in part supported by OTR3 S.A.S, the manufacturer of RGTA® (HSm4131). Authors F. Sineriz, E. Pascolo-Rebouillat, are employees of OTR3, D. Barritault is a significant OTR3 shareholder and RGTA patents inventor and co-owner. All provided technical guidance for these experiments as members of the project steering committee. However, the funding body had no influence on data acquisition, evaluation or presentation.

References

1. Nogueira RG, Jadhav AP, Haussen DC, Bonafe A, Budzik RF, Bhuva P, et al. Thrombectomy 6 to 24 hours after stroke with a mismatch between deficit and infarct. N Engl J Med. 2018; 378(1): 11–21.
2. Demaerschalk BM. Alteplase treatment in acute stroke: incorporating food and drug administration prescribing information into existing acute stroke management guide. Current Curr Atheroscler Rep. 2016; 18(8): 18–53.
3. Smith PD, Coulson-thomas VJ, Foscarin S, Kwok JCF, Fawcett JW. GAG-ing with the neuron: the role of glycosaminoglycan patterning in the central nervous system. Exp Neurol. 2015; 274(Pt B): 100-14.
4. Barritault D, Gilbert-Sirieix M, Rice KL , Siñeriz F, Papy-Garcia D, Baudouin C, et al. RGTA® or ReGeneraTing Agents mimic heparan sulfate in regenerative medicine: from concept to curing patients. Glycoconj J. 2017;34(3): 325-38.
5. Li J, Li JP, Zhang X, Lu Z, Ping S, Wei L. Expression of heparanase in vascular cells and astrocytes of the mouse brain after focal cerebral ischemia. Brain Res. 2012;1433: 137-44.
6. Takahashi H, Matsumoto H, Kumon Y, Ohnishi T, Freeman C, Imai Y et al. Expression of heparanase in nestin-positive reactive astrocytes in ischemic lesions of rat brain after transient middle cerebral artery occlusion. Neurosci Lett. 2007; 417(3): 250–4.
7. Ghuman H, Massensini AR, Donnelly J, Kim S, Medberry CJ, Badylak SF, et al. ECM hydrogel for the treatment of stroke : characterization of the host cell infiltrate. Biomaterials 2016; 91: 166–181.
8. Rouet V, Hamma-Kourbali Y, Petit E, Panagopoulou P, Katsoris P, Barritault D et al. A synthetic glycosaminoglycan mimetic binds vascular endothelial growth factor and modulates angiogenesis. J Biol Chem. 2005; 280(38): 32792–800.
9. Tong M, Zbinden MM, Hekking IJ, Vermeij M, Barritault D, van Neck JW. RGTA OTR 4120, a heparan sulfate proteoglycan mimetic, increases wound breaking strength and vasodilatory capability in healing rat full-thickness excisional wounds. Wound Repair Regen. 2008; 16(2): 294–9.
10. Blanquaert F, Barritault D, Caruelle JP. Effects of heparan-like polymers associated with growth factors on osteoblast proliferation and phenotype expression. J Biomed Mater Res. 1999; 44(1): 63–72.
11. Ikeda Y, Charef S, Ouidja MO, Barbier-Chassefière V, Sineriz F, Duchesnay A, et al. Synthesis and biological activities of a library of glycosaminoglycans mimetic oligosaccharides. Biomaterials 2011; 32(3): 769–76.
12. Mangoni M, Yue X, Morin C, Violot D, Frascogna V, Tao Y, et al. Differential effect triggered by a heparan mimetic of the RGTA family preventing oral mucositis without tumor protection. Int J Radiat Oncol Biol Phys. 2009; 74(4): 1242–50.
13. Hermann DM, Zechariah A. Implications of vascular endothelial growth factor for postischemic neurovascular remodeling. J Cereb Blood Flow Metab. 2009; 29(10): 1620–43.

14. Chuquet J, Benchenane K, Toutain J, MacKenzie ET, Roussel S, Touzani O. Selective blockade of endothelin-B receptors exacerbates ischemic brain damage in the rat. Stroke. 2002; 33(12): 3019–25
15. Quittet MS, Touzani O, Sindji L, Cayon J, Fillesoye F, Toutain J, Divoux D , et al. Effects of mesenchymal stem cell therapy, in association with pharmacologically active microcarriers releasing VEGF, in an ischaemic stroke model in the rat. Acta Biomater. 2015; 15: 77–88.
16. Schneider CA, Rasband WS, Eliceiri KW. NIH Image to ImageJ: 25 years of image analysis. Nat Methods. 2012; 9(7): 671–5.
17. Gerriets T, Stolz E, Walberer M, Müller C, Kluge A, Bachmann A, et al. Noninvasive quantification of brain edema and the space-occupying effect in rat stroke models using magnetic resonance imaging. Stroke. 2004; 35(2): 566–71.
18. Bederson JB, Pitts LH, Tsuji M, Nishimura MC, Davis RL, Bartkowski H. Rat middle cerebral artery occlusion: evaluation of the model and development of a neurologic examination. Stroke. 1986; 17(3): 472–6.
19. Freret T, Valable S, Chazalviel L, Saulnier R, Mackenzie ET, Petit E, et al. Delayed administration of deferoxamine reduces brain damage and promotes functional recovery after transient focal cerebral ischemia in the rat. Eur J Neurosci. 2006; 23(7): 1757–65.
20. De Ryck M , Van Reempts J., Borgers M, Wauquier A, Janssen PA. Photochemical stroke model: flunarizine prevents sensorimotor deficits after neocortical infarcts in rats. Stroke. 1989; 20(10): 1383–90.
21. Schallert T, Upchurch M, Lobaugh N, Farrar SB, Spirduso WW, Gilliam P, et al. Tactile extinction: distinguishing between sensorimotor and motor asymmetries in rats with unilateral nigrostriatal damage. Pharmacol Biochem Behav. 1982; 16(3): 455–62.
22. Haelewyn B, Freret T, Pacary E, Schumann-Bard P, Boulouard M, Bernaudin M, et al. Long-term evaluation of sensorimotor and mnesic behaviour following striatal NMDA-induced unilateral excitotoxic lesion in the mouse. Behav Brain Res. 2007; 178(2): 235–43.
23. Schallert T, Woodlee MT, Fleming SM. Disentangling multiple types of recovery from brain injury recovery of function. In: Pharmacology of Cerebral Ischemia, Suttgart: Medpharm Scientific Publishers, Krieglstein J and Klump S, eds, 2002: 201–16.
24. Bouet V, Boulouard M, Toutain J, Divoux D, Bernaudin M, Schumann-Bard P, et al. The adhesive removal test: a sensitive method to assess sensorimotor deficits in mice. Nat Protoc. 2009; 4(10): 1560–64.
25. Marti HJ, Bernaudin M, Bellail A, Schoch H, Euler M, Petit E, et al. Hypoxia-induced vascular endothelial growth factor expression precedes neovascularization after cerebral ischemia. Am J Pathol. 2000; 156(3): 965–76.
26. Li C, Zhang B, Zhu Y, Li Y, Liu P, Gao B, et al. Post-stroke constraint-induced movement therapy increases functional recovery, angiogenesis, and neurogenesis with enhanced expression of HIF-1 α and VEGF. Curr Neurovasc Res. 2017;14(4): 368–77.
27. Liu XS, Chopp M, Zhang RL, Hozeska-Solgot A, Gregg SC, Buller B, et al. Angiopoietin 2 mediates the differentiation and migration of neural progenitor cells in the subventricular zone after stroke. J Biol Chem. 2009; 284(34): 22680–9.
28. Hill JJ, Jin K, Mao XO, Xie L, Greenberg DA. Intracerebral chondroitinase ABC and heparan sulfate proteoglycan glypican improve outcome from chronic stroke in rats. Proc Natl Acad Sci U S A. 2012; 109(23): 9155–60.
29. Meddahi A, Brée F, Papy-Garcia D, Gautron J, Barritault D, Caruelle JP. Pharmacological studies of RGTA(11), a heparan sulfate mimetic polymer, efficient on muscle regeneration. J Biomed Mater Res. 2002; 62(4): 525–31.
30. Valable S, Montaner J, Bellail A, Berezowski V, Brillault J, Cecchelli R, et al. VEGF-induced BBB permeability is associated with an MMP-9 activity increase in cerebral ischemia: both effects decreased by Ang-1. J Cereb Blood Flow Metab. 2005; 25(11): 1491–504.
31. Desgranges P, Barritault D, Caruelle JP, Tardieu M. Transmural endothelialization of vascular prostheses is regulated in vitro by fibroblast growth factor 2 and heparan-like molecule. Int J Artif Organs. 1997; 20(10): 589–98.
32. Lindvall O, Kokaia Z. Neurogenesis following stroke affecting the adult brain. Cold Spring Harb Perspect Biol. 2015; 7(11). pii: a019034.
33. Wiltrout C, Lang B, Yan Y, Dempsey RJ, Vemuganti R. Repairing brain after stroke: a review on post-ischemic neurogenesis. Neurochem Int. 2007, 50(7-8): 1028–41.
34. Bishop JR, Schuksz M, Esko JD. Heparan sulphate proteoglycans fine-tune mammalian physiology. Nature. 2007; 446(7139): 1030–7.
35. Lanfranconi S, Locatelli F, Corti S, Candelise L, Comi GP, Baron PL, et al. Growth factors in ischemic stroke. J Cell Mol Med. 2011; 15(8): 1645–87.
36. Wang Y, Jin K, Mao XO, Xie L, Banwait S, Marti HH, Greenberg DA. VEGF-overexpressing transgenic mice show enhanced post-ischemic neurogenesis and neuromigration. J Neurosci Res. 2007; 85(4): 740–7.
37. Kim JY, Kawabori M, Yenari MA. Innate inflammatory responses in stroke: mechanisms and potential therapeutic targets. Curr Med Chem. 2014; 21(18): 2076–97.
38. Hoehn BD, Palmer TD, Steinberg GK. Neurogenesis in rats after focal cerebral ischemia is enhanced by indomethacin. Stroke. 2005; 36(12):2718-24.
39. Barritault D, Garcia-Filipe S, Zakine G. [Basement of matrix therapy in regenerative medicine by RGTA(®): from fundamental to plastic surgery]. Ann Chir Plast Esthet. 2010; 55(5): 413–20.
40. Barritault D, Desgranges P, Meddahi-Pellé A, Denoix JM, Saffar JL. RGTA®-based matrix therapy - A new branch of regenerative medicine in locomotion. Joint Bone Spine. 2017; 84(3): 283–92.
41. Zhang JM, An J. Cytokines, inflammation, and pain. Int Anesthesiol Clin. 2007; 45(2): 27–37.
42. Aurora AB, Olson EN. Immune modulation of stem cells and regeneration. Cell stem Cell. 2014; 15(1): 14–25.
43. Escartin Q, Lallam-Laroye C, Baroukh B, Morvan FO, Caruelle JP, Godeau G, et al. A new approach to treat tissue destruction in periodontitis with chemically modified dextran polymers. FASEB J. 2003; 17(6): 644–51.
44. Shichita T, Sakaguchi R, Suzuki M, Yoshimura A. Post-ischemic inflammation in the brain. Front Immunol. 2012; 3: 132.
45. Barreto G, White RE, Ouyang Y, Xu L, Giffard RG. Astrocytes: targets for neuroprotection in stroke. Cent Nerv Syst Agents Med Chem. 2011; 11(2): 164–73.
46. Faulkner JR, Herrmann JE, Woo MJ, Tansey KE, Doan NB, Sofroniew MV. Reactive astrocytes protect tissue and preserve function after spinal cord injury. J Neurosci. 2004; 24(9): 2143–55.
47. Bush TG, Puvanachandra N, Horner CH, Polito A, Ostenfeld T, Svendsen CN, et al. Leukocyte infiltration, neuronal degeneration, and neurite outgrowth after ablation of scar-forming, reactive astrocytes in adult transgenic mice. Neuron. 1999; 23(2): 297–308.